AJNR

# Quantification of Diffusivities of the Human Cervical Spinal Cord Using a 2D Single-Shot Interleaved Multisection Inner Volume Diffusion-Weighted Echo-Planar Imaging Technique

T.H. Kim, L. Zollinger, X.F. Shi, S.E. Kim, J. Rose, A.A. Patel and E.K. Jeong

*AJNR Am J Neuroradiol* published online 17 December 2009
http://www.ajnr.org/content/early/2009/12/17/ajnr.A1881.citation

Published December 17, 2009 as 10.3174/ajnr.A1881

ORIGINAL RESEARCH

# Quantification of Diffusivities of the Human Cervical Spinal Cord Using a 2D Single-Shot Interleaved Multisection Inner Volume Diffusion-Weighted Echo-Planar Imaging Technique

T.H. Kim
L. Zollinger
X.F. Shi
S.E. Kim
J. Rose
A.A. Patel
E.K. Jeong

**BACKGROUND AND PURPOSE:** DTI is a highly sensitive technique, which can detect pathology not otherwise noted with conventional imaging methods. This paper provides the atlas of reliable normative in vivo DTI parameters in the cervical spinal cord and its potential applications toward quantifying pathology.

**MATERIALS AND METHODS:** In our study, we created a reference of normal diffusivities of the cervical spinal cord by using a 2D ss-IMIV-DWEPI technique from 14 healthy volunteers and compared parameters with those in 8 patients with CSM. The 2D ss-IMIV-DWEPI technique was applied in each subject to acquire diffusion-weighted images. FA, $\lambda_{\parallel}$, and $\lambda_{\perp}$ were calculated. A reference of normal DTI indices from 12 regions of interest was created and compared with DTI indices of 8 patients.

**RESULTS:** A map of reference diffusivity values was obtained from healthy controls. We found statistically significant differences in diffusivities between healthy volunteers and patients with CSM with different severities of disease, by using FA, $\lambda_{\parallel}$, and $\lambda_{\perp}$ values.

**CONCLUSIONS:** DTI using 2D ss-IMIV-DWPEI is sensitive to spinal cord pathology. This technique can be used to detect and quantify the degree of pathology within the cervical spinal cord from multiple disease states.

**ABBREVIATIONS:** CSM = cervical spondylotic myelopathy; 2D ss-IMIV-DWEPI = 2D single-shot interleaved multisection inner volume diffusion-weighted echo-planar imaging; DTI = diffusion tensor imaging; DW = diffusion-weighted; EPI = echo-planar imaging; ETL = echo-train length; FA = fractional anisotropy; $\lambda_{\parallel}$ = longitudinal diffusivity; $\lambda_{\perp}$ = radial diffusivity; IMIV = interleaved multisection inner volume; NMG = Nurick myelopathy grading; RGB = red-green-blue; SNR= signal intensity–to-noise ratio; T2WI = T2-weighted imaging

SPINE

ORIGINAL RESEARCH

DTI is becoming a valuable surrogate measurement of the microscopic anatomy of the central nervous system. It measures both the magnitude and direction of the diffusion of water molecules by applying gradients in multiple planes. DTI can characterize white matter tracts within the brain and spinal cord by measuring alterations to the anisotropy of tissue. The measured $\lambda_{\parallel}$ is thought to be a marker for axonal disease, while the diffusion perpendicular to axonal tracts can provide information on the integrity of myelin sheaths, though direct histopathologic comparison has yet to be established.[1]

Many in vivo[2-4] DTI measurements have been conducted with the hope that they would lead to improved understanding of the pathology and ultimately improved in vivo techniques for evaluating tissue microstructure. However, as of now there is no consensus as to the in vivo technique that will provide robust, accurate, and reliable measurements that can establish a reference of normal DTI indices for the spinal cord. In addition, the clinical application of DTI in spinal cord imaging has proved difficult for the following reasons: 1) The commonly used multishot acquisition technique is highly sensitive to the physiologic motion in vivo, limiting its diagnostic accuracy, and 2) the locally varying nonlinear gradient, which is caused by the magnetic susceptibility difference at/near the vertebral bones, induces substantial geometric distortion on 2D ss-DWEPI, which is most widely used in brain DTI.

Recently, Jeong et al[5,6] reported an IMIV imaging technique that uses double inversion/refocusing radio-frequency pulses with 2D ss-DWEPI. Because this technique allows efficient DTI measurements of anatomic regions where conventional 2D ss-DWEPI has severe magnetic susceptibility distortion, the entire cervical spinal cord can be obtained in the sagittal plane within 1 interleaved imaging. The geometric distortion in 2D ss-DWEPI is proportional to the FOV in the phase-encoding direction; therefore, 2D ss-IMIV-DWEPI reduces the susceptibility distortion by reducing the spatial coverage in the phase-encoding direction and allows DTI measurements from nearly any localized region of the body, many

Received June 9, 2009; accepted after revision August 17.

From the Department of Radiology (T.H.K., L.Z., S.E.K., E.K.J.), Utah Center for Advanced Imaging Research (T.H.K., X.F.S., S.E.K., E.K.J.), and Departments of Physics (X.F.S.), Neurology (J.R.), and Orthopedic Surgery (A.A.P.), University of Utah, Salt Lake City, Utah.

This work was supported by the Cervical Spine Research Society Starter Grant 2008, the National Multiple Sclerosis Society, the Cumming Foundation, the Benning Foundation, the Margolis Foundation, and National Institutes of Health grants R21NS052424 and R21EB005705.

Please address correspondence to Eun-Kee Jeong, PhD, Utah Center for Advanced Imaging Research, Radiology, University of Utah, 729 Arapeen Dr, Salt Lake City, UT 84108-1218; e-mail: ekj@ucair.med.utah.edu

Indicates article with supplemental on-line tables.

Indicates open access to non-subscribers at www.ajnr.org

DOI 10.3174/ajnr.A1881

**Limited demographics from 8 patients with a history of CSM and SNR of T2WI**

| Patients | Age (yr) | Sex | Conventional MR Imaging: Levels of Stenosis | SNR | NMG |
|---|---|---|---|---|---|
| P1 | 61 | M | C4/C5, C5/C6, C6/C7 | 16.29 | 3 |
| P2 | 78 | F | C3/C4, C4/C5, C5/C6 | 19.52 | 4 |
| P3 | 43 | M | C5/C6, C6/C7 | 13.24 | 4 |
| P4 | 64 | M | C3/C4, C4/C5, C5/C6, C6/C7 | 26.01 | 2 |
| P5 | 48 | M | C4/C5, C5/C6 | 13.90 | 3 |
| P6 | 64 | M | C4/C5, C5/C6 | 11.27 | 2 |
| P7 | 48 | M | C3/C4, C4/C5, C5/C6, C7/T1 | 26.27 | 2 |
| P8 | 70 | F | C4/C5, C5/C6, C6/C7 | 21.74 | 3 |

of which cannot be currently studied with other available DTI techniques.

In this article, we will present our efforts to improve the clinical utility of DTI in the cervical spinal cord by quantifying diffusivities of healthy volunteers and comparing the values with those of patients with CSM. For this study, we used 2D ss-DWEPI with the IMIV imaging technique and a custom-made cervical spinal cord coil.

## Materials and Methods

### *Subjects and DTI*

Control subjects were recruited on a volunteer basis. Each of the control subjects was interviewed to exclude any history of cervical spondylosis, myelopathy, previous spine surgery, spinal cord trauma, or other neurodegenerative diseases. A total of 14 healthy control subjects were included.

Patients with CSM were also recruited, on a volunteer basis, from the practice of 1 author (A.A.P.). All patients were diagnosed with CSM by clinical examination and conventional MR imaging. The degree of clinical information available for the patients was significantly limited by the boundaries of our research-approval status. Exclusion criteria were the following: noncervical sources of myelopathy, infection, tumor, history of central neurodegenerative diseases (eg, multiple sclerosis), and a history of cranial white matter diseases. The severity of myelopathy was assessed and scored by the NMG scale: 0, normal function; 1, no walking impairment; 2, mild walking impairment, able to continue working; 3, walking impairment, unable to work; 4, immobilized in a wheelchair or bed. A total of 8 patients were included, each with a history of chronic myelopathy (>1-year duration of symptoms) related to prior trauma or progressive spondylolysis.

The MR imaging experiments were performed on a 3T whole-body MR imaging system (Trio; Siemens Medical Solutions, Erlangen, Germany) with Avanto gradients (45 mT/m strength and 150 T/m/s slew rate). Characteristics of controls (average age, 34 years) and patients with CSM (average age, 59.5 years) are listed in the Table.

Our imaging protocol was approved by the institutional review board, and informed consent was obtained from the participants. T2WI by using 2D turbo spin-echo was performed to verify the location of the cervical spinal cord. The imaging parameters were the following: TR = 4000 ms, TE = 114 ms, in-plane resolution = 0.75 × 0.75 $mm^2$, section thickness = 1.5 mm, ETL = 19, and receiver bandwidth = 248 Hz/pixel.

Each of the control subjects was imaged by using a custom-made cervical spinal cord coil. It consisted of 8 rectangular coils and covered the posterior neck from the occiput to the T2 vertebra. Among 14 healthy volunteers, 6 were rescanned with a clinical coil routinely used at our institution. It consisted of a 12-channel receive-only head coil (Siemens Medical Solutions) and a spine coil with an anterior neck coil assembly (USA Instruments, Aurora, Ohio). All of the patients with CSM were imaged once by using only the clinical coil.

The imaging parameters of 2D ss-IMIV-DWEPI were the following: TR = 4000 ms, TE = 65 ms, imaging matrix = 160 × 40, imaging resolution = 1.5 × 1.5 × 2.0 $mm^3$, $b$=500 s/$mm^2$, ETL = 41, receiver bandwidth = 1078 Hz/pixel, and 10 interleaved sections. Diffusion-weighted gradients were applied in 12 noncollinear directions. Total scanning time for the DTI acquisition was 7 minutes.

### *Data Analysis and Physical Parameters*

The acquired DTI dataset was processed pixel-by-pixel by using home-made DTI processing software written in Interactive Data Language (ITT Visual Information Solutions, Boulder, Colorado). First, 3 eigenvalues ($\lambda_1$, $\lambda_2$, $\lambda_3$) and eigenvectors were calculated. $\lambda_{\parallel}$ and $\lambda_{\perp}$ were obtained from 3 eigenvalues by using

$$1) \qquad \lambda_{\parallel} = \lambda_1$$

$$\lambda_{\perp} = (\lambda_2 + \lambda_3)/2.$$

Here, $\lambda_1$ is the principal diffusivity with the largest value in each image pixel. The degree of anisotropy was presented by using the anisotropy index FA,[7] which is defined as

$$2) \quad FA = \sqrt{3[(\lambda_1 - \lambda_{mean})^2 + (\lambda_2 - \lambda_{mean})^2 + (\lambda_3 - \lambda_{mean}{}^2)]} \,/\, \sqrt{2(\lambda_1^2 + \lambda_2^2 + \lambda_3^2)},$$

where $\lambda_{mean}$ indicates the mean diffusivity. FA values from 0 (completely isotropic) to 1 (completely anisotropic) indicate the degree of structural anisotropy. The data were processed to extract the RGB fiber map. The RGB map indicates the direction of the principal eigenvector: blue represents the superior-to-inferior axis; green, left-to-right; and red, anterior-to-posterior.

Regions of interest were selected from the FA map by using the anatomy and cord morphology from the T2WI as a reference. Twelve regions of interest were selected from a sagittal section through the midline of the cord to maximize the number of pixels analyzed within the dorsal columns on each participant, spanning C1–C7. Region-of-interest selection is demonstrated in Fig 1. We applied the whole-cord analysis,[2] including both the white and gray matter as well as regions of cord corresponding to disk levels. The separation of the gray and white matter was not attempted due to challenges of image resolution. The regions of interest were delineated to exclude approximately 2 voxels from the edge of the cord along the anterior and posterior margins. Care was taken to account for variant morphology of the cervical cord among subjects to ensure accuracy and reliability. No standardized techniques were used to normalize the cervical cords among subjects. Regions of interest were, therefore, manually delineated within the dorsal white matter columns to maximize the size of evaluated cord. Average $\lambda_{\parallel}$, $\lambda_{\perp}$, and FA were calculated from the multiple regions of interest along the entire cervical spinal cord. Group statistics were calculated for each of the DTI parameters and SNR. The group means and SDs were obtained by using the subject means. Quantitative statistical comparison of anisotropic parameters from the controls and patients was conducted by using normal distributions and a $P$ value of .05.

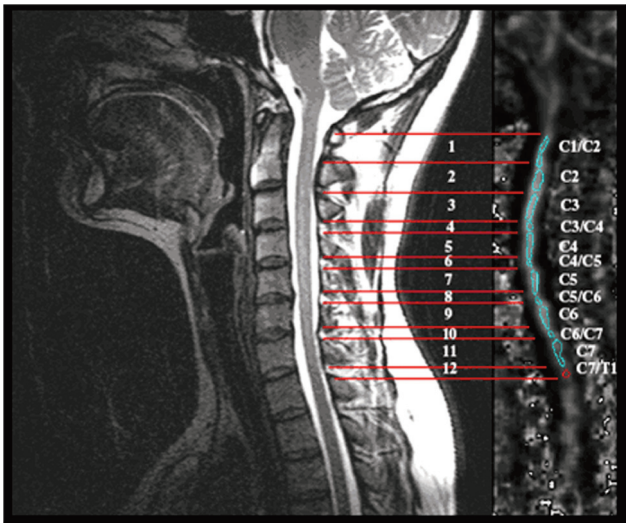


**Fig 1.** Sagittal T2WI of the cervical spinal cord from a healthy volunteer demonstrating the method of region-of-interest selection and relative spinal levels.

## Results

Figure 1 displays a sagittal T2WI of the normal cervical spinal cord demonstrating the region-of-interest selection and relative spinal-level selection from the occiput through C7. The SNR in the T2WI of the 14 healthy controls with the specially constructed coil was measured as 38 ± 11.9. The same value for the clinical coil from the 6 healthy controls was 20 ± 8.4.

Figure 2 includes the diffusion properties of healthy controls obtained by using 2 different radio-frequency coils. The red line represents the results from the custom-made coil from the 14 volunteers, and the black line is the data from the 6 volunteers who were scanned a second time with the clinical coil. There are no significant differences in the obtained values between the 2 coils by using a paired-samples *t* test. The *P* values for each of the indices were as follows: $P = .095$ (Fig 2*A*), .295 (Fig 2*B*), and .812 (Fig 2*C*). This figure shows that the custom-made coil provided less variation and higher values in $\lambda_{\|}$ and FA compared with the clinical coil. Nearly equivalent $\lambda_{\|}$ and $\lambda_{\perp}$ values were obtained across the healthy volunteers for each cervical spinal level.

Figure 3 shows the colored scaled FA maps and RGB fiber map of 3 contiguous sections from a healthy control and a patient with CSM. FA maps from the healthy subjects generally show uniform values across the entire cervical spine. In contrast, FA maps of the patients with CSM demonstrate abrupt changes in FA values at sites of pathology. The RGB map from a healthy subject in Fig 3*A* shows uniform blue filling on the cord, which indicates that the direction of fiber is the same as the direction of the principal water diffusion (head-foot). We observed color degradation and decreased FA values in the patients. These results were also in concert with findings from conventional T2WIs as shown in Fig 3.

The quantitative statistical comparison of diffusivity properties from the patients and controls is reported in On-line Tables 1–3. Using the mean value from each region of interest based on the clinical coil, we assumed a normal distribution. With a $P < .05$, any measured values from the patients with CSM that were outside the 95% confidence interval were deemed significantly different from those of the healthy patients on a level-by-level basis. The regions of interest from the occiput through C3 were obtained, though not included in the level-by-level analysis due to the low SNR from all subjects. On-line Tables 1–3 shows that multiple areas within the cords of the patients with CSM had significantly different values of $\lambda_{\|}$, $\lambda_{\perp}$, and FA compared with those of the healthy controls at the same spinal levels based on a *P* value of .05.

Additional quantitative comparison of DTI parameters for 8 patients and the group mean values of the healthy volunteers are presented in Fig 4, by using the NMG. There is a significant variation from the normal values at the levels where there is significant spinal stenosis. Direct-level testing of the patients' disabilities was not available due to limitations of institutional review board approval; however, there was general agreement with the aberrancies of the diffusivity indices and their degree of clinical impairment.

## Discussion

There are numerous and novel approaches to in vivo DTI spinal cord imaging as discussed previously.[4,8-10] However, they also have several limitations in providing robust and reliable measurements of DTI. The greatest limitations have been related to the scanning time for DTI acquisition, distortion, and motion-related artifacts. Previous work has excluded cord evaluation at the level of intervertebral disks because of the significant susceptibility artifacts.[2] In this report, we present the DTI results from in vivo cervical spinal cord imaging of both healthy volunteers and patients with CSM while maintaining a short imaging time of 7 minutes. The 2D ss-IMIV-DWEPI technique allowed efficient interleaved multisection imaging with fewer magnetic susceptibility distortion artifacts, affording an increase in the quality of images with a limited FOV.

The regions of interest were selected within the dorsal columns to maximize the size of the area evaluated while minimizing the acquisition time compared with previous axial techniques.[2,10,11] Although whole-cord analysis in the sagittal plane cannot avoid more partial volume effects compared with axial techniques because of the cord anatomy, a scanning time of 7 minutes with a high in-section resolution is clinically feasible for patients. Corticospinal tract evaluation within the lateral columns, while desirable, is technically challenging due to the long imaging time needed to maintain adequate SNR and FOV.

Prior studies have been conducted describing DTI of the cervical spinal cord by using imaging acquired in the sagittal plane with the section thickness ranging from 4 to 6 mm.[9,12,13] These techniques had decreased in-section resolution, which caused partial volume effects. Although in-plane resolution is relatively high, partial volume effects from the gray matter may not be ignored. In our study, we minimized the section thickness to reduce the gray-white matter partial volume. We were able to obtain ~8 clean sagittal sections of entire cord in a cross-sectional direction by using the small FOV with the IMIV technique to decrease the error related to partial volume averaging, which has been problematic in previous experiments.

Initially, the custom-made coil was developed to improve image quality, SNR, and the overall reliability of our data, in the hope that it could be used on all research subjects. Our

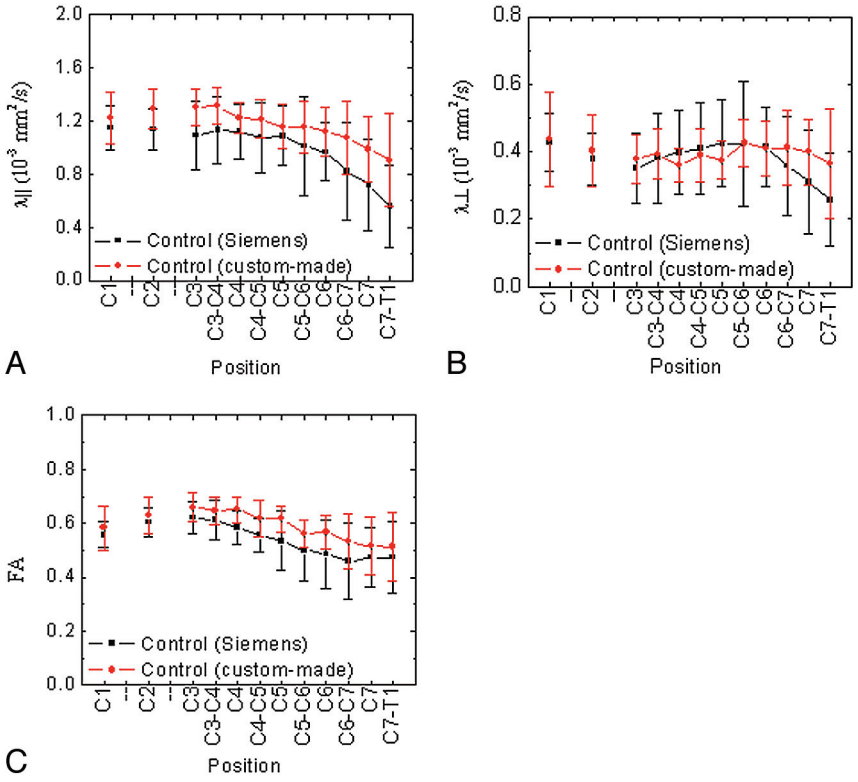


**Fig 2.** DTI parameters: longitudinal (*A*) and transversal diffusivities (*B*) and FA (*C*) of the cervical spinal cord of healthy controls by using 2 different coils (custom-made coil, 14 controls; clinical coil, 6 controls).

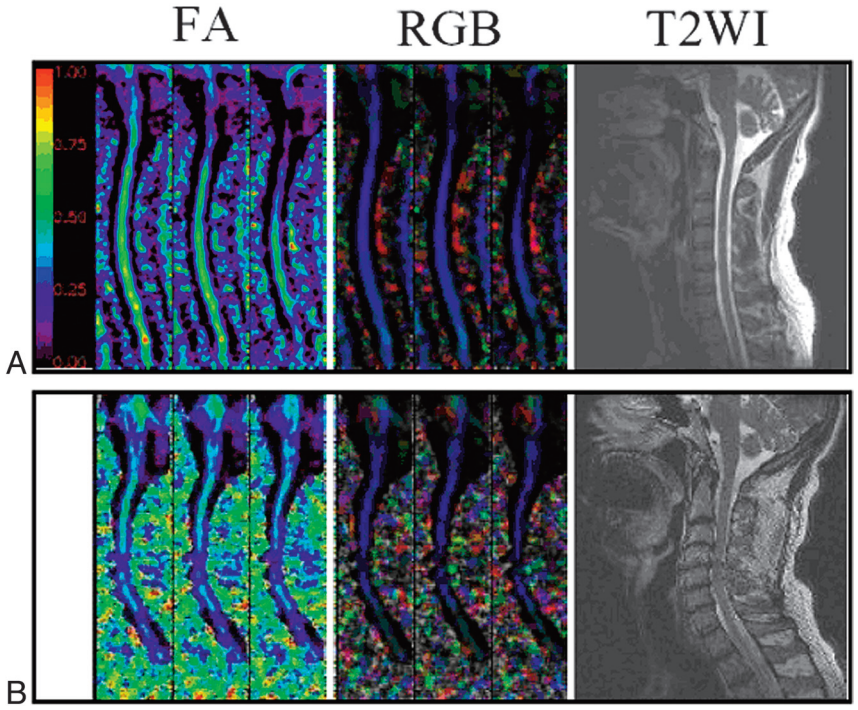


**Fig 3.** *A*, FA and RGB maps of 3 contiguous sections and T2WI of the center section from a healthy volunteer. The FA map shows uniform values throughout the cord. The RGB map demonstrates that the principal direction of diffusivity is along the longitudinal direction, as depicted in blue. The T2WI shows a normal cervical cord without atrophy of lesions. *B*, FA, RGB map, and T2WI from patient 2 with severe diskogenic disease and stenosis at C3/4, C4/5, and C5/6. There is a loss of FA values at the sites of stenosis. The RGB map shows admixing of colors at similar levels.

dedicated coil maintained an SNR ~2 times better than the clinical coil, but its use was limited by the body habitus of our subjects. We, therefore, used both the custom-made coil and the clinical coil to image the healthy controls. The validity of the custom-made coil was demonstrated by comparing DTI indices with those acquired by using the clinical coil array. We

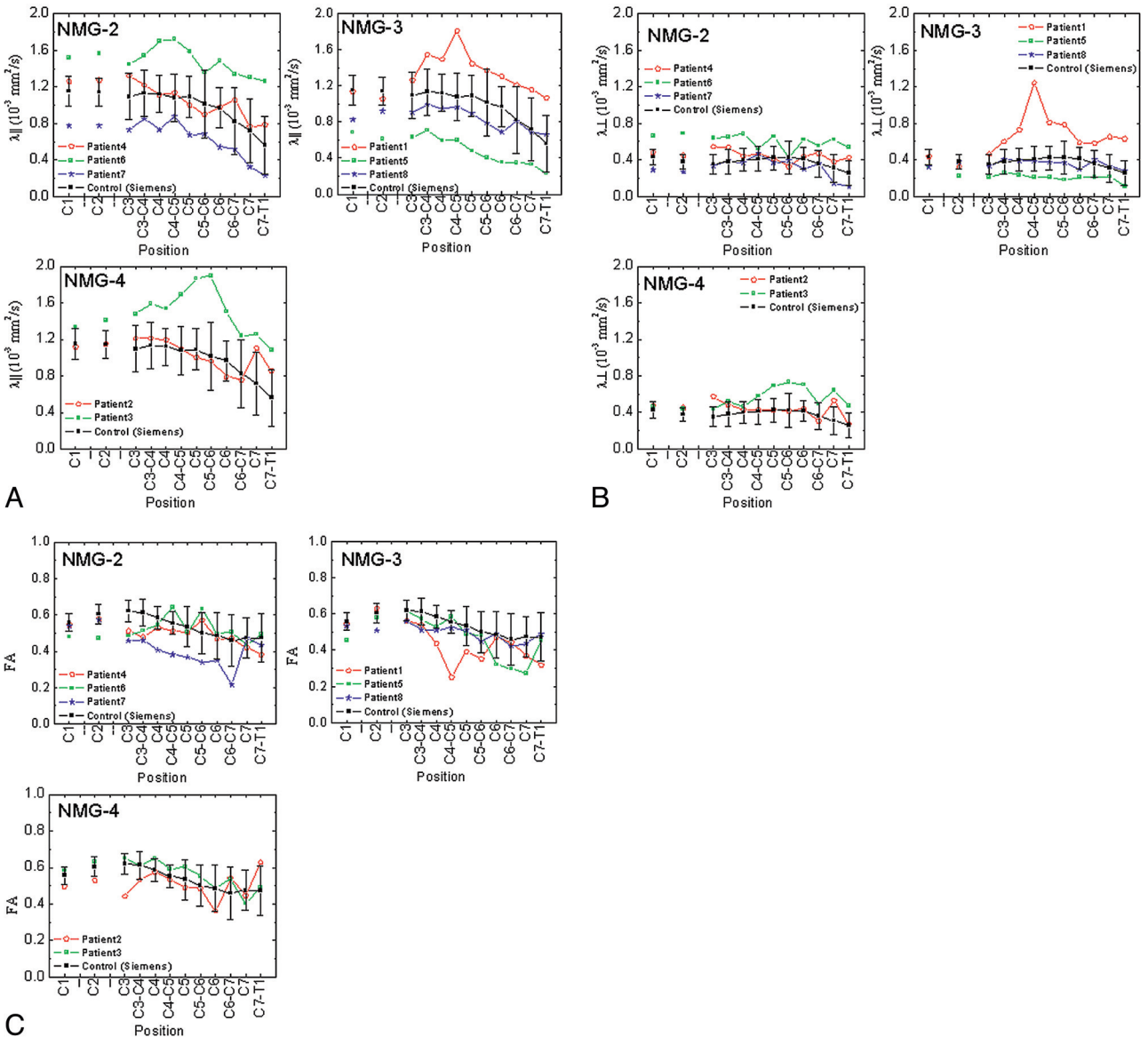


**Fig 4.** Longitudinal diffusivity (*A*), radial diffusivity (*B*), and FA (*C*) from patients as a function of NMG.

confirmed the importance of high SNR according to the Monte Carlo simulation performed by Pierpaoli and Basser,[14] which showed the radical changes of $\lambda_{\parallel}$ and $\lambda_{\perp}$ at a low SNR. In Fig 2, the clinical coil shows a large variation and, especially, a significant decrease in the indices below the C6 vertebral level due to a low SNR. In contrast, the dedicated coil provided almost constant values of indices over the length of the cervical spinal cord, in good agreement with those in the previous reports.[2,10]

In this report, we demonstrate the reliability of our DTI measurements by using the 2D ss-IMIV DWEPI technique for healthy controls. With the custom-made coil, the mean diffusivities over the entire cord were $\lambda_{\parallel} = 1.17 \times 10^{-3}$ ($mm^2/s$), $\lambda_{\perp} = 0.40 \times 10^{-3}$ ($mm^2/s$), and FA = 0.59. With the clinical coil, they were $\lambda_{\parallel} = 0.99 \times 10^{-3}$, $\lambda_{\perp} = 0.38 \times 10^{-3}$, and FA = 0.54. Our results are in fair concordance with the report of Wheeler-Kingshott et al[10] ($\lambda_{\parallel}$, $\lambda_{\perp}$: 1.648, $0.570 \times 10^{-3}$ $mm^2/s$ and FA: 0.61) and the report of Ellingson et al[11] ($\lambda_1$, $\lambda_2$, and $\lambda_3$: 1.2–.5, 0.6–0.7, and $0.4–0.5 \times 10^{-3}$ $mm^2/s$ and FA: 0.5–0.6) by using axial plane images. We observed a downward trend in all the diffusivities toward the lower cervical cord, as demonstrated previously. However, there is no consensus as to what values are normal. Rossi et al[4] reported a range of FA values from 0.69 to 0.79 in the center of the cord at the fourth cervical vertebra by using axial plane imaging, and Ries et al[3] reported an FA of 0.83 at the center of the spinal cord using sagittal plane imaging. The FA from our sagittal acquisition ranged from 0.46 to 0.61, which is very similar to the findings of Ellingson et al (0.5–0.6).[11]

While maintaining an adequate SNR ($20 \pm 8.4$ for healthy controls by using the clinical coil), we established reference values and created individual quantitative maps of $\lambda_{\parallel}$, $\lambda_{\perp}$, and FA for each level of the cervical spinal cord of healthy volunteers. These data were considered as a reference for the patients with CSM (SNR = $18.5 \pm 5.8$). The diffusivities obtained from the patients with CSM were deemed abnormal on a level-by-level basis on the basis of a *P* value of .05. General trends were observed at the levels of disease across all patients

compared with the control subjects. The $\lambda_{\parallel}$ and $\lambda_{\perp}$ were both increased, while FA trended low. Fifty percent of the patients had significantly lower FA values than the reference values within diseased regions of interest, as shown in Fig 4.

The FA has been used in previous experiments as a rough estimate of microstructural abnormalities,[15] but we suggest that these data must be used in addition to $\lambda_{\parallel}$ and $\lambda_{\perp}$ values to understand potential causes of abnormalities. With patient 5 as an example, the FA values were within the normal range in regions of diseased cord, while the $\lambda_{\parallel}$ and $\lambda_{\perp}$ values were abnormal, likely from the low SNR that affected the entire acquisition. As shown in Fig 3, patient 3 has a significant change in $\lambda_{\parallel}$ and $\lambda_{\perp}$, while the FA values show insignificant variation. This is probably because the FA value is a scaled representation of $\lambda_{\parallel}$ and $\lambda_{\perp}$. The changes in $\lambda_{\parallel}$ and $\lambda_{\perp}$ can cancel each other in the calculation of FA.

Some patients with CSM had aberrantly increased $\lambda_{\parallel}$ values at multiple levels, without complete agreement with findings from conventional MR imaging. For instance, patient 1 had severe stenosis at C4/C5, C5/C6, and C6/C7; however $\lambda_{\parallel}$ was significantly different from the reference values only at C4/C5. This patient had elevated $\lambda_{\perp}$, in accord with the measured $\lambda_{\parallel}$. Patient 3 had elevated $\lambda_{\parallel}$ at the C4 through C6 and elevated $\lambda_{\perp}$ at levels C5, C6, and C7. This was in contrast to patient 4 who showed no significant changes in any parameter despite multilevel disease found with conventional imaging.

The differences in DTI indices we demonstrated between patients with CSM and healthy volunteers are similar to those in the previous reports. Facon et al[8] found a statistically significant difference in the measured FA of healthy volunteers versus patients with known disease at the same level (0.67 and 0.74, respectively). Mamata et al[13] reported that 54% of patients with spondylosis ($n = 79$) showed an FA decreased from normal cords (0.66–0.70). Ellingson et al[11] reported the diffusion properties of the patients with chronic spinal cord injury based on the relative distance from a spinal cord lesion. While FA was low at the level of the lesion, they reported a gradual change in values as a function of distance from the site for the patients.

In addition to measured values, the improved quality of the DTI by using the 2D ss-IMIV-DWEPI technique allows the identification of pathology based on abnormalities identified with RGB maps. We were able to match the shape of our subjects' spinal cords with FA and RGB maps and to maintain consistent region-of-interest mapping to allow direct comparison. Figure 3 demonstrates the high-quality DTI and a close correlation between conventional MR imaging findings and DTI results. Areas of stenosis can be clearly identified on FA and RGB maps. Altered FA values are consistent with areas of deformation of the cord, which then result in changes to the measured anisotropy. By comparing measured diffusivities between patients and controls, we found that trends in the DTI values were consistent with conventional MR imaging findings and the available clinical information.

As of now, histologic correlation with abnormal $\lambda_{\parallel}$ has been theorized to represent axonal pathology, while $\lambda_{\perp}$ is considered to be a marker of myelin integrity.[1] By comparing measured diffusion properties between patients and controls, we found that trends in the DTI values were consistent with conventional MR imaging findings and the available clinical information. Additional studies are underway at our institution that allow direct histologic correlation with both MR imaging and DTI in the ex vivo setting.

## Conclusions

The DTI data from healthy volunteers by using the 2D ss-IMIV-DWEPI technique allowed us to generate a normal reference map of diffusivity values. The reference DTI metrics proved useful in comparison with pathology found with conventional MR imaging performed on patients with CSM. By developing a normal DTI atlas, we found numerous potential clinical applications in which we may quantify the degree of microstructural impairment within the spinal cord and relate it to clinical disability and treatment effects.

## References


1. Song S-K, Sun S-W, Ramsbottom MJ, et al. **Dysmyelination revealed through MRI as increased radial (but unchanged axial) diffusion of water.** *Neuroimage* 2002;17:1429–36
2. Ellingson BM, Ulmer JL, Kurpad SN, et al. **Diffusion tensor MR imaging of the neurologically intact human spinal cord.** *AJNR Am J Neuroradiol* 2008;29:1279–84
3. Ries M, Jones RA, Dousset V, et al. **Diffusion tensor MRI of the spinal cord.** *Magn Reson Med* 2000;44:884–92
4. Rossi C, Boss A, Steidle G, et al. **Water diffusion anisotropy in white and gray matter of the human spinal cord.** *J Magn Reson Imaging* 2008;27:476–82
5. Jeong E-K, Kim S-E, Guo J, et al. **High-resolution DTI with 2D interleaved multislice reduced FOV single-shot diffusion-weighted EPI (2D ss-rFOV-DWEPI).** *Magn Reson Med* 2005;54:1575–79
6. Jeong E-K, Kim S-E, Kholmovski EG, et al. **High-resolution DTI of a localized volume using 3D single-shot diffusion-weighted stimulated echo-planar imaging (3D ss-DWSTEPI).** *Magn Reson Med* 2006;56:1173–81
7. Bihan DL, Mangin J-F, Poupon C, et al. **Diffusion tensor imaging: concepts and applications.** *J Magn Reson Imaging* 2001;13:534–46
8. Facon D, Ozanne A, Fillard P, et al. **MR diffusion tensor imaging and fiber tracking in spinal cord compression.** *AJNR Am J Neuroradiol* 2005;26:1587–94
9. Hori M, Okubo T, Aoki S, et al. **Line scan diffusion tensor MRI at low magnetic field strength: feasibility study of cervical spondylotic myelopathy in an early clinical stage.** *J Magn Reson Imaging* 2006;23:183–88
10. Wheeler-Kingshott CA, Hickman SJ, Parker GJ, et al. **Investigating cervical spinal cord structure using axial diffusion tensor imaging.** *Neuroimage* 2002;16:93–102
11. Ellingson BM, Ulmer JL, Kurpad SN, et al. **Diffusion tensor MR imaging in chronic spinal cord injury**. *AJNR Am J Neuroradiol* 2008;29:1976–82. Epub 2008 Aug 21
12. Clark CA, Barker GJ, Tofts PS. **Magnetic resonance diffusion imaging of the human cervical spinal cord in vivo.** *Magn Reson Med* 1999;41:1269–73
13. Mamata H, Jolesz FA, Maier SE. **Apparent diffusion coefficient and fractional anisotropy in spinal cord: age and cervical spondylosis-related changes.** *J Magn Reson Imaging* 2005;22:38–43
14. Pierpaoli C, Basser PJ. **Toward a quantitative assessment of diffusion anisotropy.** *Magn Reson Med* 1996;36:893–906
15. Agosta F, Benedetti B, Rocca MA, et al. **Quantification of cervical cord pathology in primary progressive MS using diffusion tensor MRI.** *Neurology* 2005;64:631–35